

Accommodation mechanism of InN nanocolumns grown on Si(111) substrates by molecular beam epitaxy

J. Grandal,^{a)} M. A. Sánchez-García, and E. Calleja

ISOM, Universidad Politécnica de Madrid, Ciudad Universitaria, s/n, 28040 Madrid, Spain and
Departamento de Ingeniería Electrónica, ETSI Telecomunicación, Universidad Politécnica de Madrid,
Ciudad Universitaria, s/n, 28040 Madrid, Spain

E. Luna and A. Trampert

Paul-Drude-Institut für Festkörperelektronik, Hausvogteiplatz 5-7, 10117 Berlin, Germany

(Received 28 April 2007; accepted 15 June 2007; published online 9 July 2007)

High quality InN nanocolumns have been grown by molecular beam epitaxy on bare and AlN-buffered Si(111) substrates. The accommodation mechanism of the InN nanocolumns to the substrate was studied by transmission electron microscopy. Samples grown on AlN-buffered Si(111) show abrupt interfaces between the nanocolumns and the buffer layer, where an array of periodically spaced misfit dislocations develops. Samples grown on bare Si(111) exhibit a thin Si_xN_y at the InN nanocolumn/substrate interface because of Si nitridation. The Si_xN_y thickness and roughness may affect the nanocolumn relative alignment to the substrate. In all cases, InN nanocolumns grow strain- and defect-free. © 2007 American Institute of Physics. [DOI: 10.1063/1.2756293]

InN has attracted much attention in the last few years due to its potential application for long wavelength optoelectronic devices, especially once its band gap value was settled to be 0.7 eV.^{1,2} InN is also a good candidate for high power/high frequency devices due to a small electron effective mass and a high electron drift velocity.

Good quality InN layers are difficult to grow because of the low dissociation temperature of InN and the lack of an appropriate substrate. Dissociation can be avoided by growing at low enough temperatures by molecular beam epitaxy. The generation of extended defects during heteroepitaxial growth on mismatched substrates can be eased using different types of buffer layers that accommodate the mismatch.

Very high crystal quality InN nanocolumns are found to be defect-free and strain-free,³ allowing for a reliable study of basic material properties. In this case, the use of buffer layers is not as critical as for InN layers, as it was also reported for GaN nanocolumns.⁴ InN nanocolumns are very attractive as building blocks for optoelectronic devices due to their high emission efficiency.

This work reports on the accommodation mechanism of InN nanocolumns grown by plasma-assisted molecular beam epitaxy (PAMBE) on Si(111) substrates, either bare or buffered with a high temperature (HT) AlN buffer. The main advantage of Si(111) substrates, aside from their low cost, crystal quality, doping capabilities, cleavability, and thermal conductivity (three times larger than sapphire), relies on the lowest lattice and thermal mismatch with InN among the common substrates used to grow III-nitrides.

The PAMBE system used in this work was equipped with a rf-plasma source (Applied Veeco UNI-Bulb) providing active nitrogen and standard Knudsen cells for In and Al. A detailed report on the growth system can be found elsewhere.⁵ Si(111) substrates were heated in the growth chamber at 800 °C for 30 min to remove the native oxide. Upon temperature decrease to 760 °C, a clear 7×7 surface reconstruction, typical of Si(111) orientation, showed up in-

dicating a full desorption of the native oxide. *In situ* growth monitoring was performed by reflection high energy electron diffraction (RHEED). The morphology and heights of InN samples were checked by scanning electron microscopy (SEM) images taken with a JEOL JSM-5800 microscope. Photoluminescence (PL) spectra were taken with a Hamamatsu P4638 PbS photodetector. High resolution transmission electron microscopy (HRTEM) images were obtained with a JEOL JEM-3010 microscope operating at 300 kV. Cross-sectional specimens were prepared by standard methods of mechanical grinding, dimpling, and Ar-ion beam milling in a cold stage unit to minimize sample damage.

The effective III/V flux ratio, together with the growth temperature, controls the layer structure.⁶ While both the III/V ratio and the growth temperature affect the layer morphology (compact versus columnar), temperature also enhances In diffusion leading to different layer morphologies, or even hindering the growth.⁷ When InN nanocolumns are grown at temperatures close to the onset of InN dissociation (550 °C) a strong diffusion of In adatoms upward the sidewalls of the nanocolumns enhances the lateral growth and leads to conical or pyramidal shapes [Fig. 1(a)].

InN nanocolumns were grown on bare and on AlN-buffered Si(111) to determine the role of the different interfaces on the lattice mismatch accommodation. Growth on

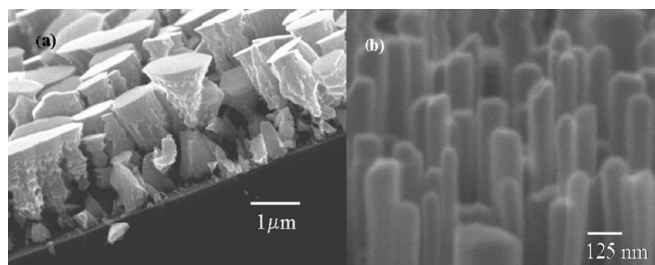


FIG. 1. (a) SEM image of pyramid-shaped InN nanocolumns grown close to the dissociation temperature (550 °C). (b) SEM image of InN nanocolumns grown at optimal temperature (475 °C).

^{a)}FAX: +34 91 336 73 23; electronic mail: jgrandal@die.upm.es

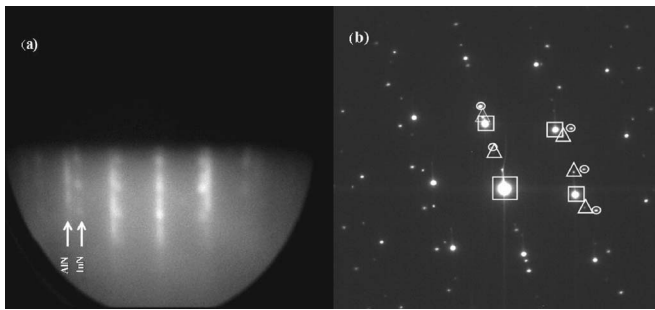


FIG. 2. (a) RHEED pattern of InN nanocolumns superimposed to the AlN-buffer one. (b) SAED image revealing three different diffraction patterns corresponding to Si(111) (squares), AlN buffer (circles), and InN nanocolumns (triangles).

HT-AlN-buffered Si(111) was preceded by depositing a few monolayers of metallic Al at high temperature. Afterward, the AlN buffer layer was then grown at 780 °C at a rate as low as 200 nm/h to minimize surface roughness according to the established optimal process.⁸ A streaky 1×1 RHEED pattern indicated a two-dimensional growth mode. Once the buffer layer is grown, the growth is stopped to decrease the temperature down to 475 °C, the optimal one for InN.⁷ When InN nanocolumnar growth starts, the RHEED pattern shows clearly the superposition of both signatures from the nanocolumn (spotty) and the buffer layer (streaky) [Fig. 2(a)].

The growth of InN nanocolumns on bare Si(111) was also performed at 475 °C. The RHEED pattern evolves from concentric rings, at the early growth stage, to rings gradually segmented as the growth proceeds. After 30 min, well defined and bright thin segments lying on concentric rings are observed until the growth ends.

SEM images revealed isolated InN nanocolumns with an average diameter of 80–120 nm in both cases. PL spectra measured at room temperature in InN nanocolumns show a single emission peak at 0.72 eV with no other contributions at higher energies. PL dependence on temperature and excitation power suggests that the emission corresponds to a band-edge recombination.⁶ No significant differences were observed in the PL emission of the InN nanocolumns grown on AlN-buffered or bare Si(111).

When InN nanocolumns are grown on bare Si(111) a thin amorphous Si_xN_y layer develops at the interface, as shown in Fig. 3(b). When the Si_xN_y layer is very thin

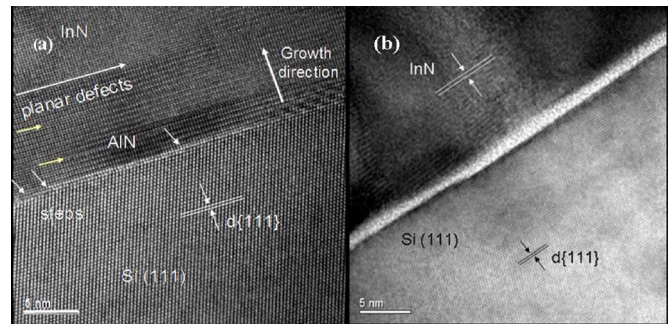


FIG. 3. (a) Cross-sectional HRTEM image of the AlN/Si(111) interface where step and planar defects are clearly seen. (b) Cross-sectional HRTEM image of the thin Si_xN_y layer developing at the interface between InN nanocolumns and the bare Si(111).

(<3 nm), a perfect alignment of the nanocolumn with its c axis perpendicular to the substrate is observed. Additionally, the in-plane epitaxial relationship between the Si(111) and the InN nanocolumns is maintained in some cases. However, for thicker and rough (i.e., steplike) Si_xN_y interlayers, the epitaxial relation is lost and thus the InN nanocolumns grow misoriented and tilted with respect to the substrate.

On the other hand, HRTEM images reveal surface steps at the AlN/Si(111) interface, already present at the Si(111) surface, that induce planar defects inside the AlN layer [Fig. 3(a)]. However, the interface between the InN nanocolumns and the AlN buffer looks atomically flat and abrupt and the nanocolumn volume is free of extended defects [Fig. 4(a)]. Selected area electron diffraction (SAED) measurements reveal three different diffraction patterns [Fig. 2(b)], which correspond to the Si substrate (squares), the AlN buffer layer (circles), and the InN nanocolumns (triangles), respectively. The close relationship between the three patterns indicates a perfect epitaxial alignment, i.e., $\text{Si}(111) \parallel \text{AlN}(0001) \parallel \text{InN}(0001)$ and $\text{Si}[110] \parallel \text{AlN}[11\bar{2}0] \parallel \text{InN}[11\bar{2}0]$. SAED patterns also show that both the AlN buffer layer and the InN nanocolumns are strain-free, as it is also corroborated by Raman spectroscopy measurements performed in this set of samples, to be published in another manuscript. This fact requires the strain accommodation by misfit dislocations, as it was observed in InN nanocolumns grown on GaN/ $\text{Al}_2\text{O}_3(0001)$ substrates⁹ and AlN layers grown on Si(111) substrates.¹⁰ Figure 4(b) shows the Fourier power spectrum of the HRTEM lattice

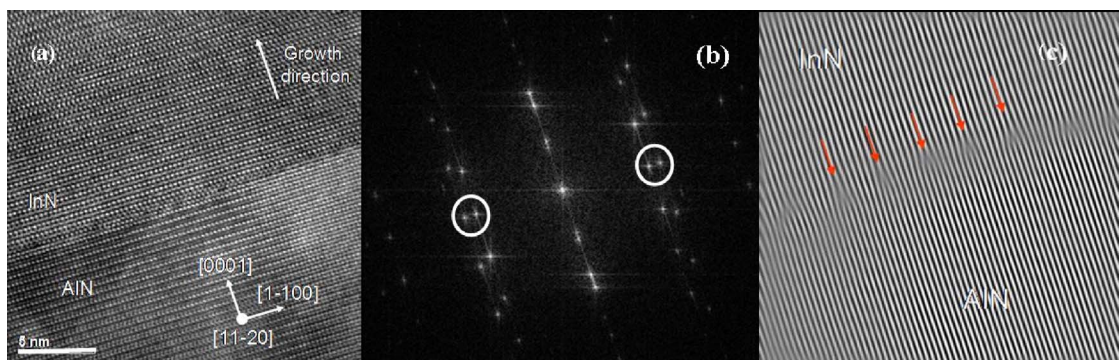


FIG. 4. (a) Cross-sectional HRTEM image revealing an atomically flat and abrupt interface between the AlN buffer layer and the InN nanocolumns. (b) Fourier power spectrum of the lattice image in (a). The two sets of spots observed correspond to the InN nanocolumns and HT-AlN buffer, respectively. The $\pm(01\bar{1}0)$ reflections contributing to the Bragg-filtered image of (c) are also shown. (c) Bragg filtered HRTEM image revealing an array of periodically spaced misfit dislocations at the interface between the AlN buffer layer and the InN nanocolumns.

image in Fig. 4(a), where the two sets of spots observed correspond to the InN nanocolumns and the AlN buffer, respectively. The Fourier-filtered image [Fig. 4(c)] reproducing lattice fringes only, which correspond to the $\pm(01\bar{1}0)$ reflections (selected spots in Fig. 4(b)), reveals how the mismatch between the InN and the AlN is relaxed by an array of misfit dislocations periodically spaced. These dislocations are only present at the InN/AlN interface with no threading arms passing into the nanocolumns, which therefore grow free of extended defects.

In summary, high crystal quality InN nanocolumns were grown either on AlN-buffered or bare Si(111) substrates. In the first case the InN/AlN interfaces were abrupt, showing a periodic array of misfit dislocations that relieved the accumulated strain. HRTEM analysis of the InN nanocolumns grown on bare Si(111) substrates revealed thin layers at the InN/Si(111) produced by Si nitridation. The thickness and flatness of the Si_xN_y layer may affect the relative alignment of the nanocolumns with the substrate. In all cases, InN nanocolumns were defect-free and strain-free, with a very high crystal quality.

The authors would like to thank H. v. Kiedrowski and A. Pfeiffer for their assistance with the TEM sample prepara-

tion. This work was partially funded by the Spanish Ministry of Education, Project No. TEC 2004-05698-C02-01.

- ¹V. Yu. Davydov, A. A. Klochikhin, R. P. Seisyan, V. V. Emtsev, S. V. Ivanov, F. Bechstedt, J. Furthmüller, H. Harima, A. V. Mudryi, J. Aderhold, O. Semchinova, and J. Graul, *Phys. Status Solidi B* **229**, R1 (2002).
- ²J. Wu, W. Walukiewicz, K. M. Yu, J. W. Ager III, E. E. Haller, H. Lu, W. J. Schaff, Y. Saito, and Y. Nanishi, *Appl. Phys. Lett.* **80**, 3967 (2002).
- ³X. Wang, S. B. Che, Y. Ishitani, and A. Yoshikawa, *Phys. Status Solidi C* **3**, 1561 (2006).
- ⁴J. Ristic, M. A. Sánchez-García, J. M. Ulloa, E. Calleja, J. Sánchez-Páramo, J. M. Calleja, U. Jahn, A. Trampert, and K. Ploog, *Phys. Status Solidi B* **234**, 717 (2002).
- ⁵M. A. Sánchez-García, E. Calleja, E. Monroy, F. J. Sanchez, F. Calle, E. Muñoz, and R. Beresford, *J. Cryst. Growth* **183**, 23 (1998).
- ⁶J. Grandal, M. A. Sánchez-García, F. Calle, and E. Calleja, *Phys. Status Solidi C* **2**, 2289 (2005).
- ⁷J. Grandal and M. A. Sánchez-García, *J. Cryst. Growth* **278**, 373 (2005).
- ⁸E. Calleja, M. A. Sánchez-García, F. J. Sánchez, F. Calle, F. B. Naranjo, E. Muñoz, S. I. Molina, A. M. Sánchez, F. J. Pacheco, and R. García, *J. Cryst. Growth* **201/202**, 296 (1999).
- ⁹Th. Kehagias, A. Delimitis, Ph. Komninou, E. Iliopoulos, E. Dimakis, A. Georgakilas, and G. Nouet, *Appl. Phys. Lett.* **86**, 151905 (2005).
- ¹⁰R. Liu, F. Ponce, A. Dadgar, and A. Krost, *Appl. Phys. Lett.* **86**, 860 (2003).